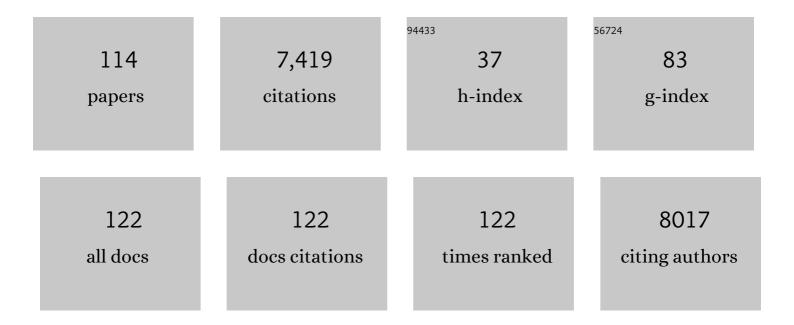
List of Publications by Year in descending order

Source: https://exaly.com/author-pdf/3353749/publications.pdf Version: 2024-02-01



#	Article	IF	CITATIONS
1	Recent Advances in Zinc Enzymology. Chemical Reviews, 1996, 96, 2375-2434.	47.7	1,323
2	Cellular function and molecular structure of ecto-nucleotidases. Purinergic Signalling, 2012, 8, 437-502.	2.2	850
3	Two-Metal Ion Catalysis in Enzymatic Acyl- and Phosphoryl-Transfer Reactions. Angewandte Chemie International Edition in English, 1996, 35, 2024-2055.	4.4	595
4	Mechanism of Fe(III) – Zn(II) Purple Acid Phosphatase Based on Crystal Structures. Journal of Molecular Biology, 1996, 259, 737-748.	4.2	342
5	Insectâ€Derived Prolineâ€Rich Antimicrobial Peptides Kill Bacteria by Inhibiting Bacterial Protein Translation at the 70 S Ribosome. Angewandte Chemie - International Edition, 2014, 53, 12236-12239.	13.8	195
6	Structural and functional studies on a thermostable polyethylene terephthalate degrading hydrolase from Thermobifida fusca. Applied Microbiology and Biotechnology, 2014, 98, 7815-7823.	3.6	191
7	Crystal Structure of the Human Ecto-5′-Nucleotidase (CD73): Insights into the Regulation of Purinergic Signaling. Structure, 2012, 20, 2161-2173.	3.3	164
8	Ecto-5'-nucleotidase: Structure function relationships. Purinergic Signalling, 2006, 2, 343-350.	2.2	159
9	Transition State Analog L-Leucinephosphonic Acid Bound to Bovine Lens Leucine Aminopeptidase: X-ray Structure at 1.65 .ANG. Resolution in a New Crystal Form. Biochemistry, 1995, 34, 9200-9210.	2.5	146
10	Vaspin inhibits kallikrein 7 by serpin mechanism. Cellular and Molecular Life Sciences, 2013, 70, 2569-2583.	5.4	125
11	Crystal structure of the plasmid maintenance system Â/Â: Functional mechanism of toxin and inactivation by Â2Â2 complex formation. Proceedings of the National Academy of Sciences of the United States of America, 2003, 100, 1661-1666.	7.1	119
12	X-ray structure of aminopeptidase A from Escherichia coli and a model for the nucleoprotein complex in Xer site-specific recombination. EMBO Journal, 1999, 18, 4513-4522.	7.8	114
13	X-ray structure of the Escherichia coli periplasmic 5'-nucleotidase containing a dimetal catalytic site. , 1999, 6, 448-453.		111
14	α,β-Methylene-ADP (AOPCP) Derivatives and Analogues: Development of Potent and Selective <i>ecto</i> -5′-Nucleotidase (CD73) Inhibitors. Journal of Medicinal Chemistry, 2015, 58, 6248-6263.	6.4	110
15	The X-ray Crystal Structure of Human β-Hexosaminidase B Provides New Insights into Sandhoff Disease. Journal of Molecular Biology, 2003, 328, 669-681.	4.2	109
16	Structural Studies on the Forward and Reverse Binding Modes of Peptides to the Chaperone DnaK. Journal of Molecular Biology, 2013, 425, 2463-2479.	4.2	104
17	Enzymatische Acyl―und Phosphoryltransferreaktionen unter Beteiligung von zwei Metallionen. Angewandte Chemie, 1996, 108, 2158-2191.	2.0	103
18	A bicarbonate ion as a general base in the mechanism of peptide hydrolysis by dizinc leucine aminopeptidase. Proceedings of the National Academy of Sciences of the United States of America, 1999, 96, 11151-11155.	7.1	100

#	Article	IF	CITATIONS
19	Crystal structure of amylomaltase from Thermus aquaticus, a glycosyltransferase catalysing the production of large cyclic glucans. Journal of Molecular Biology, 2000, 296, 873-886.	4.2	96
20	Mechanism of hydrolysis of phosphate esters by the dimetal center of 5′-nucleotidase based on crystal structures. Journal of Molecular Biology, 2001, 309, 239-254.	4.2	96
21	Api88 Is a Novel Antibacterial Designer Peptide To Treat Systemic Infections with Multidrug-Resistant Gram-Negative Pathogens. ACS Chemical Biology, 2012, 7, 1281-1291.	3.4	94
22	Mechanisms of catalysis and allosteric regulation of yeast chorismate mutase from crystal structures. Structure, 1997, 5, 1437-1452.	3.3	93
23	Structural relationship between the mammalian Fe(III)-Fe(II) and the Fe(III)-Zn(II) plant purple acid phosphatases. FEBS Letters, 1995, 367, 56-60.	2.8	88
24	Calcium-sensing receptor-mediated NLRP3 inflammasome response to calciprotein particles drives inflammation in rheumatoid arthritis. Nature Communications, 2020, 11, 4243.	12.8	79
25	Rational Design of Oncocin Derivatives with Superior Protease Stabilities and Antibacterial Activities Based on the Highâ€Resolution Structure of the Oncocinâ€DnaK Complex. ChemBioChem, 2011, 12, 874-876.	2.6	77
26	Crystal Structures of Recombinant Human Purple Acid Phosphatase With and Without an Inhibitory Conformation of the Repression Loop. Journal of Molecular Biology, 2005, 351, 233-246.	4.2	73
27	Crystallographic Evidence for a Domain Motion in Rat Nucleoside Triphosphate Diphosphohydrolase (NTPDase) 1. Journal of Molecular Biology, 2012, 415, 288-306.	4.2	73
28	Structural insight into signal conversion and inactivation by NTPDase2 in purinergic signaling. Proceedings of the National Academy of Sciences of the United States of America, 2008, 105, 6882-6887.	7.1	71
29	Low Carbon Footprint Recycling of Post onsumer PET Plastic with a Metagenomic Polyester Hydrolase. ChemSusChem, 2022, 15, .	6.8	70
30	Structure and allosteric regulation of eukaryotic 6-phosphofructokinases. Biological Chemistry, 2013, 394, 977-993.	2.5	58
31	Crystal Structure of Thermotoga maritima α-Glucosidase AglA Defines a New Clan of NAD+-dependent Glycosidases. Journal of Biological Chemistry, 2003, 278, 19151-19158.	3.4	56
32	Discovery of AB680: A Potent and Selective Inhibitor of CD73. Journal of Medicinal Chemistry, 2020, 63, 11448-11468.	6.4	52
33	E. coli 5′-nucleotidase undergoes a hinge-bending domain rotation resembling a ball-and-socket motion. Journal of Molecular Biology, 2001, 309, 255-266.	4.2	50
34	Crystal structure of the T state of allosteric yeast chorismate mutase and comparison with the R state Proceedings of the National Academy of Sciences of the United States of America, 1996, 93, 3330-3334.	7.1	46
35	Surface supercharged human enteropeptidase light chain shows improved solubility and refolding yield. Protein Engineering, Design and Selection, 2011, 24, 261-268.	2.1	45
36	Crystallographic Snapshots along the Reaction Pathway of Nucleoside Triphosphate Diphosphohydrolases. Structure, 2013, 21, 1460-1475.	3.3	44

#	Article	IF	CITATIONS
37	X-ray structure of acarbose bound to amylomaltase from Thermus aquaticus. FEBS Journal, 2000, 267, 6903-6913.	0.2	43
38	Amylose recognition and ring-size determination of amylomaltase. Science Advances, 2017, 3, e1601386.	10.3	42
39	A glutamate residue in the catalytic center of the yeast chorismate mutase restricts enzyme activity to acidic conditions. Proceedings of the National Academy of Sciences of the United States of America, 1997, 94, 8491-8496.	7.1	38
40	2-Substituted α,β-Methylene-ADP Derivatives: Potent Competitive Ecto-5′-nucleotidase (CD73) Inhibitors with Variable Binding Modes. Journal of Medicinal Chemistry, 2020, 63, 2941-2957.	6.4	37
41	Characterization of Rat NTPDase1, -2, and -3 Ectodomains Refolded from Bacterial Inclusion Bodies. Biochemistry, 2007, 46, 11945-11956.	2.5	34
42	Discovery of Potent and Selective Non-Nucleotide Small Molecule Inhibitors of CD73. Journal of Medicinal Chemistry, 2020, 63, 3935-3955.	6.4	34
43	Xâ€Ray Coâ€Crystal Structure Guides the Way to Subnanomolar Competitive Ectoâ€5′â€Nucleotidase (CD73) Inhibitors for Cancer Immunotherapy. Advanced Therapeutics, 2019, 2, 1900075.	3.2	33
44	Crystal structure and spectroscopic characterization of cesium vanadium sulfate CsV(SO4)2. Evidence for an electronic Raman transition. Inorganic Chemistry, 1993, 32, 4714-4720.	4.0	30
45	A Large Hinge Bending Domain Rotation Is Necessary for the Catalytic Function ofEscherichia coli5â€~-Nucleotidaseâ€. Biochemistry, 2005, 44, 2244-2252.	2.5	30
46	Reinforced HNA Backbone Hydration in the Crystal Structure of a Decameric HNA/RNA Hybrid. Journal of the American Chemical Society, 2005, 127, 2937-2943.	13.7	30
47	Structural Identification of DnaK Binding Sites within Bovine and Sheep Bactenecin Bac7. Protein and Peptide Letters, 2014, 21, 407-412.	0.9	30
48	Crystallization and preliminary crystallographic data of purple acid phosphatase from red kidney bean. Journal of Molecular Biology, 1992, 224, 511-513.	4.2	27
49	Identification of residues important for NAD+binding by theThermotoga maritimaα-glucosidase AgIA, a member of glycoside hydrolase family 4. FEBS Letters, 2002, 517, 267-271.	2.8	26
50	Crystal Structure of Hexokinase KlHxk1 of Kluyveromyces lactis. Journal of Biological Chemistry, 2010, 285, 41019-41033.	3.4	26
51	Functional Linkage of Adenine Nucleotide Binding Sites in Mammalian Muscle 6-Phosphofructokinase. Journal of Biological Chemistry, 2012, 287, 17546-17553.	3.4	25
52	Structures of <i>Legionella pneumophila</i> NTPDase1 in complex with polyoxometallates. Acta Crystallographica Section D: Biological Crystallography, 2014, 70, 1147-1154.	2.5	25
53	Crystal structure of NTPDase2 in complex with the sulfoanthraquinone inhibitor PSB-071. Journal of Structural Biology, 2014, 185, 336-341.	2.8	25
54	Trapping a 96° domain rotation in two distinct conformations by engineered disulfide bridges. Protein Science, 2004, 13, 1811-1822.	7.6	24

#	Article	IF	CITATIONS
55	Cosubstrateâ€induced dynamics of Dâ€3â€hydroxybutyrate dehydrogenase from <i>Pseudomonas putida</i> . FEBS Journal, 2007, 274, 5767-5779.	4.7	24
56	Structural Basis of the Stereospecificity of Bacterial B12-dependent 2-Hydroxyisobutyryl-CoA Mutase. Journal of Biological Chemistry, 2015, 290, 9727-9737.	3.4	23
57	Functional impact of intramolecular cleavage and dissociation of adhesion G protein–coupled receptor GPR133 (ADGRD1) on canonical signaling. Journal of Biological Chemistry, 2021, 296, 100798.	3.4	23
58	Crystal structure of human platelet phosphofructokinase-1 locked in an activated conformation. Biochemical Journal, 2015, 469, 421-432.	3.7	22
59	Structural Insight into Activation Mechanism of Toxoplasma gondii Nucleoside Triphosphate Diphosphohydrolases by Disulfide Reduction*. Journal of Biological Chemistry, 2012, 287, 3051-3066.	3.4	21
60	Proline-rich Antimicrobial Peptides Optimized for Binding to Escherichia coli Chaperone DnaK. Protein and Peptide Letters, 2016, 23, 1061-1071.	0.9	21
61	Crystallization and preliminary X-ray diffraction studies of the â^ŠÎ¶ addiction system encoded byStreptococcus pyogenesplasmid pSM19035. Acta Crystallographica Section D: Biological Crystallography, 2001, 57, 745-747.	2.5	19
62	An Artificial Imine Reductase based on the Ribonucleaseâ€S Scaffold. ChemCatChem, 2014, 6, 736-740.	3.7	19
63	Characterization of the Domain Orientations of E.Âcoli 5′-Nucleotidase by Fitting an Ensemble of Conformers to DEER Distance Distributions. Structure, 2016, 24, 43-56.	3.3	19
64	Structure and function of the abasic site specificity pocket of an AP endonuclease from Archaeoglobus fulgidus. DNA Repair, 2009, 8, 219-231.	2.8	18
65	Active-Site Mobility Revealed by the Crystal Structure of Arylmalonate Decarboxylase from Bordetella bronchiseptica. Journal of Molecular Biology, 2008, 377, 386-394.	4.2	17
66	A unique serpin P1′ glutamate and a conserved β-sheet C arginine are key residues for activity, protease recognition and stability of serpinA12 (vaspin). Biochemical Journal, 2015, 470, 357-367.	3.7	17
67	Surfaceâ€Binding Peptide Facilitates Electricityâ€Driven NADPHâ€Free Cytochrome P450 Catalysis. ChemCatChem, 2018, 10, 525-530.	3.7	17
68	Discovery of Potent and Selective Methylenephosphonic Acid CD73 Inhibitors. Journal of Medicinal Chemistry, 2021, 64, 845-860.	6.4	17
69	X-ray structure of acarbose bound to amylomaltase from Thermus aquaticus . Implications for the synthesis of large cyclic glucans. FEBS Journal, 2000, 267, 6903-6913.	0.2	17
70	Understanding the Structural Basis of Adhesion GPCR Functions. Handbook of Experimental Pharmacology, 2016, 234, 67-82.	1.8	16
71	Structure of DNA helicase RepA in complex with sulfate at 1.95â€Ã resolution implicates structural changes to an `open' form. Acta Crystallographica Section D: Biological Crystallography, 2003, 59, 815-822.	2.5	14
72	Molecular architecture and structural basis of allosteric regulation of eukaryotic phosphofructokinases. FASEB Journal, 2011, 25, 89-98.	0.5	14

#	Article	IF	CITATIONS
73	Basic Residues of β-Sheet A Contribute to Heparin Binding and Activation of Vaspin (Serpin A12). Journal of Biological Chemistry, 2017, 292, 994-1004.	3.4	14
74	Kallikrein-related peptidase 14 is the second KLK protease targeted by the serpin vaspin. Biological Chemistry, 2018, 399, 1079-1084.	2.5	14
75	Ribosomal Targetâ€Binding Sites of Antimicrobial Peptides Api137 and Onc112 Are Conserved among Pathogens Indicating New Lead Structures To Develop Novel Broadâ€5pectrum Antibiotics. ChemBioChem, 2020, 21, 2628-2634.	2.6	14
76	Crystal structure of a supercharged variant of the human enteropeptidase light chain. Proteins: Structure, Function and Bioinformatics, 2012, 80, 1907-1910.	2.6	13
77	Contribution of the two domains of <i>E. coli</i> 5′â€nucleotidase to substrate specificity and catalysis. FEBS Letters, 2013, 587, 460-466.	2.8	13
78	New crystal forms of NTPDase1 from the bacterium <i>Legionella pneumophila</i> . Acta Crystallographica Section F: Structural Biology Communications, 2013, 69, 257-262.	0.7	13
79	Fluorine ontaining 6,7â€Ðialkoxybiarylâ€Based Inhibitors for Phosphodiesteraseâ€10 A: Synthesis and ir vitro Evaluation of Inhibitory Potency, Selectivity, and Metabolism. ChemMedChem, 2014, 9, 1476-1487.	¹ 3.2	13
80	Glycosylation of human vaspin (SERPINA12) and its impact on serpin activity, heparin binding and thermal stability. Biochimica Et Biophysica Acta - Proteins and Proteomics, 2017, 1865, 1188-1194.	2.3	12
81	Structures of 2-Hydroxyisobutyric Acid-CoA Ligase Reveal Determinants of Substrate Specificity and Describe a Multi-Conformational Catalytic Cycle. Journal of Molecular Biology, 2019, 431, 2747-2761.	4.2	12
82	Expression and purification of the ligand-binding domain of peroxisome proliferator-activated receptor alpha (PPARα). Protein Expression and Purification, 2008, 62, 185-189.	1.3	10
83	Protein surface charge of trypsinogen changes its activation pattern. BMC Biotechnology, 2014, 14, 109.	3.3	10
84	Recombinant expression of a unique chloromuconolactone dehalogenase ClcF from Rhodococcus opacus 1CP and identification of catalytically relevant residues by mutational analysis. Archives of Biochemistry and Biophysics, 2012, 526, 69-77.	3.0	9
85	The crystal structure of <i>Toxoplasma gondii</i> nucleoside triphosphate diphosphohydrolase 1 represents a conformational intermediate in the reductive activation mechanism of the tetrameric enzyme. Proteins: Structure, Function and Bioinformatics, 2013, 81, 1271-1276.	2.6	9
86	Localization and orientation of heavy-atom cluster compounds in protein crystals using molecular replacement. Acta Crystallographica Section D: Biological Crystallography, 2013, 69, 284-297.	2.5	9
87	Crystal structure and substrate binding mode of ectonucleotide phosphodiesterase/pyrophosphatase-3 (NPP3). Scientific Reports, 2018, 8, 10874.	3.3	9
88	Leucyl aminopeptidase (animal). , 2004, , 896-901.		9
89	Regulatory Function of Hexokinase 2 in Glucose Signaling in Saccharomyces cerevisiae. Journal of Biological Chemistry, 2016, 291, 16477.	3.4	8
90	Structural Studies on the Inhibitory Binding Mode of Aromatic Coumarinic Esters to Human Kallikrein-Related Peptidase 7. Journal of Medicinal Chemistry, 2020, 63, 5723-5733.	6.4	8

#	Article	IF	CITATIONS
91	Substrate binding modes of purine and pyrimidine nucleotides to human ecto-5′-nucleotidase (CD73) and inhibition by their bisphosphonic acid derivatives. Purinergic Signalling, 2021, 17, 693-704.	2.2	8
92	Crystal structure of cleaved vaspin (serpinA12). Biological Chemistry, 2016, 397, 111-123.	2.5	7
93	RNase T1 Variant RV Cleaves Single-Stranded RNA after Purines Due to Specific Recognition by the Asn46 Side Chain Amide. Biochemistry, 2004, 43, 2854-2862.	2.5	6
94	Crystallization and preliminary X-ray analysis of the open form of human ecto-5′-nucleotidase (CD73). Acta Crystallographica Section F: Structural Biology Communications, 2012, 68, 1545-1549.	0.7	6
95	Analysis of a rare functional truncating mutation rs61757459 in vaspin (SERPINA12) on circulating vaspin levels. Journal of Molecular Medicine, 2013, 91, 1285-1292.	3.9	6
96	In vivo phosphorylation and in vitro autophosphorylation-inactivation of Kluyveromyces lactis hexokinase KlHxk1. Biochemical and Biophysical Research Communications, 2013, 435, 313-318.	2.1	6
97	Crystal structure and catalytic mechanism of chloromuconolactone dehalogenase <scp>ClcF</scp> from <i><scp>R</scp>hodococcus opacus</i> 1 <scp>CP</scp> . Molecular Microbiology, 2013, 88, 254-267.	2.5	6
98	Membrane Phospholipids and Polyphosphates as Cofactors and Binding Molecules of SERPINA12 (vaspin). Molecules, 2020, 25, 1992.	3.8	6
99	The ATP/ADP Substrate Specificity Switch between <i>Toxoplasma gondii</i> NTPDase1 and NTPDase3 is Caused by an Altered Mode of Binding of the Substrate Base. ChemBioChem, 2013, 14, 2292-2300.	2.6	5
100	Leucyl Aminopeptidase (Animal). , 2013, , 1465-1470.		5
101	Crystallization and preliminary crystallographic analysis of human muscle phosphofructokinase, the main regulator of glycolysis. Acta Crystallographica Section F, Structural Biology Communications, 2014, 70, 578-582.	0.8	5
102	Structure–Activity Relationship of 3-Methylcytidine-5′-α,β-methylenediphosphates as CD73 Inhibitors. Journal of Medicinal Chemistry, 2022, 65, 2409-2433.	6.4	5
103	X-Ray Structure Analysis of Methane Monooxygenase: An Important Step toward Understanding the Oxidation of Methane in Biological Systems. Angewandte Chemie International Edition in English, 1994, 33, 841-843.	4.4	4
104	Röntgenstrukturanalyse der Methanâ€Monooxygenase: ein wichtiger Beitrag zum Verstädnis der Oxidation von Methan in biologischen Systemen. Angewandte Chemie, 1994, 106, 889-891.	2.0	3
105	Crystallization and preliminary characterization of chloromuconolactone dehalogenase fromRhodococcus opacus1CP. Acta Crystallographica Section F: Structural Biology Communications, 2012, 68, 591-595.	0.7	3
106	Crystal Structure of Apo―and Metalated Thiolate containing RNase S as Structural Basis for the Design of Artificial Metalloenzymes by Peptideâ€Protein Complementation. Zeitschrift Fur Anorganische Und Allgemeine Chemie, 2013, 639, 2395-2400.	1.2	3
107	Mono-ADP-ribosylation sites of human CD73 inhibit its adenosine-generating enzymatic activity. Purinergic Signalling, 2022, 18, 115-121.	2.2	3
108	Yeast chorismate and other allosteric enzymes. Pure and Applied Chemistry, 1998, 70, 527-531.	1.9	2

#	Article	IF	CITATIONS
109	Crystallization and preliminary X-ray characterization of two thermostable DNA nucleases. Acta Crystallographica Section F: Structural Biology Communications, 2006, 62, 1290-1293.	0.7	2
110	Crystallization and preliminary X-ray diffraction studies of hexokinase KlHxk1 fromKluyveromyces lactis. Acta Crystallographica Section F: Structural Biology Communications, 2007, 63, 430-433.	0.7	2
111	Crystallization of ectonucleotide phosphodiesterase/pyrophosphatase-3 and orientation of the SMB domains in the full-length ectodomain. Acta Crystallographica Section F, Structural Biology Communications, 2018, 74, 696-703.	0.8	2
112	Posttranslational Incorporation of Noncanonical Amino Acids in the RNase S System by Semisynthetic Protein Assembly. Methods in Molecular Biology, 2014, 1216, 71-87.	0.9	1
113	Biochemie und Molekularbiologie 2003. Nachrichten Aus Der Chemie, 2004, 52, 292-305.	0.0	0
114	Structure activity relationship of 3â€methylcytidineâ€5'â€Î±,βâ€methylenediphosphates as CD73 inhibitors. Journal, 2022, 36, .	FASEB	0